Lehigh University
Lehigh Preserve

Fritz Laboratory Reports   Civil and Environmental Engineering

1962

Fatigue tests of welded plate girders, February 1962

P. B. Cooper

B. T. Yen

Follow this and additional works at: http://preserve.lehigh.edu/engr-civil-environmental-fritz-lab-reports

FATIGUE TESTS OF WELDED PLATE GIRDERS

by

B. T. Yen

and

Peter B. Cooper

Lehigh University

Fritz Engineering Laboratory Report No. 251.26

February 1962

SYNOPSIS

Tests on two welded plate girders were conducted to observe the behavior under fatigue loading of girders with very slender webs and to obtain preliminary data for planning further investigation. The girders, 40 feet long, 50 inches deep, with 3/16-inch webs, were subjected primarily to shear in such a manner that, under static loading, a shear failure would occur. A load range of half-maximum to maximum was used. With maximum loads of 83% and 71% of the respective static strengths, tension field action developed which contributed to the formation of fatigue cracks in the girder webs. While further study is being planned, the test results suggest the applicability of the design recommendations[1] to highway bridges.

Errata
(F.L. Report 251.26)

P.11, 4th line, Fig. 4C.

P.21, 11th line, fluctuation was 0.2 inch or more.

Fig. 11, deflection scale should be 1/2" instead of 1".

Fig. 13, deflection scale should be 0.4" instead of 1".

251.26

TABLE OF CONTENTS

INTRODUCTION

Fatigue tests on two full-size welded plate girders were conducted at Lehigh University in 1961. The purpose of this paper is to report the results obtained from these tests.

Prior to the tests, an extensive theoretical and experimental investigation of the static behavior of welded plate girders was carried out.[2,3,4,5] A suggested application of the results to the design of plate girders has been presented in the form of design recommendations[1] which have been incorporated recently in the new AISC Specification[6]. One of the objectives of the fatigue tests to be described here was to investigate the applicability of these recommendations to girders subjected to repeated loading.

The accomplishing of this objective necessitated the testing of full-size specimens, thus eliminating the possible influence of a size effect which could be introduced by the use of model girders. Although it was estimated that the equipment available at Fritz Engineering Laboratory would be adequate for the desired tests, a second objective was to check on the applicability of the equipment and setup.

Of course it was not expected that tests on only two specimens would provide enough data to solve the entire problem of the fatigue strength of plate girders. It was

anticipated that the two tests, besides serving to check the test setup and the equipment, would be of great assistance in the planning of future fatigue tests.

As reported recently,[4] tension field action is an important factor in the evaluation of the shear carrying capacity of slender web girders. However, is tension field action of greater concern than all the other problems which are encountered in the fatigue of welded plate girders? To investigate this, pronounced shear loading had to be selected.

As a preliminary to a presentation and discussion of the test results, the test girders and test conditions will first be described.

I. THE GIRDERS

1.1 Design of Girders

The two girders are shown in Fig. 1. Girder F1 was
designed with a geometric configuration which would not be
permitted under the design recommendations[1] while girder
F2 conformed to the recommended rules. Thin webs were used
to emphasize the effect of shear loading. For comparison
the two girders were the same as shear girders G6 and G7 in
Ref. 2 except for the flange and stiffener sizes.

As can be seen from Fig. 1, each girder had relatively
strong flanges of 1 inch thickness continuous through the
entire girder. Cover plates of the same thickness were
added to the flanges at reaction points. These thicker
plates were to provide girders (stiffer than girders G6 and
G7) to keep within the stroke limitations of the test equip-
ment and to reduce the flange stresses so as to decrease the
possibility of a flange failure. The 50-inch deep web, un-
like the continuous flanges, was composed of 3/8-inch plates
at the ends and a 3/16-inch plate in the center portion where
failure was expected to occur. The central section is termed
the test section (Fig. 2).

The two girders differed only in the spacing of inter-
mediate transverse stiffeners within the test section.

Girder F2 had a spacing of 50 inches, or a ratio of panel
length to web depth (aspect ratio) of 1.0. Girder F1, with
an aspect ratio of 1.5, had two identical panels of 75 inches
in the test section. Since F1 had longer panels than F2 and
hence a lower allowable average shear stress in the web, it
would have a shorter fatigue life than F2 if both girders
were subjected to the same magnitude of loading.

Intermediate transverse stiffeners were 3 x 1/4-inch
plates welded continuously to both sides of the web and to
the compression flange. The cutting short of the stiffeners
adjacent to the tension flange and the seemingly small size
of the stiffeners as compared to practice were such that they
were the minimum required by the design recommendations.[1]

1.2 Girder Dimensions and Material Properties

For all practical purposes, the nominal dimensions shown
in Fig. 1 were also the actual dimensions. The actual thick-
ness and width of each component plate, however, varied some-
what from the nominal sizes. Therefore, prior to assembly,
a short length was cut off at the ends of each plate for size
measurements as well as for test coupons. In this way the
actual dimensions as summarized in Table 1 were determined.
The web depth of 50 inches was maintained during fabrication.

At least one coupon was cut from each flange, web, and cover plate in the longitudinal direction unless two or more plates came from the same slab. In that case, a single coupon was considered sufficient for the entire slab. All coupon dimensions conformed to ASTM requirements for plates over 3/16-inch thickness. The results of the coupon tests are shown in Table 2 along with the chemical analysis of the heats from which the plates originated. All material conformed to ASTM 373-58T, but the plates were selected with the aim of obtaining the same yield point for the web and the flanges.

A more complete description of the methods used to determine girder dimensions as well as material and girder properties can be found in Ref. 2.

1.3 Welding Sequence

To obtain test specimens representative of structures actually used, the girders were shop fabricated under the same conditions and by the same welding procedure as would be used on actual girders. Except for the weld sizes, the latest AWS Specifications were followed. The rule used for determining weld sizes was that the sum of the throat dimensions of the two opposite fillet welds should equal the thickness of the thinner of the two plates to be joined. The weld sizes, welding sequence, and details used are presented in Tables 3a and 3b.

It should be mentioned that the intermediate and bear-
ing stiffeners of girder Fl were initially welded to the web
plate using the submerged-arc process. Due to difficulty in
positioning the welding machine, some of the welds laid down
were unsatisfactory. These welds were chipped out and re-
placed manually. The corresponding welds on girder F2 were
placed manually as indicated in the table.

1.4 Cross-Sectional Constants and Reference Values

In Table 4 are listed several values for reference and
comparison. The first group contains the cross-sectional
constants for the test section: the moment of inertia I, the
section modulus S, and the first moment Q of a half section
about the neutral axis. These constants were calculated using
ordinary beam theory.

The next group lists the aspect ratio (panel length to
web depth) α, the web slenderness ratio (web depth to thick-
ness) β, the web buckling stress τ_{cr}, and the corresponding
web buckling load P_{cr}, as computed according to the linear
buckling theory.

The yield load P_y, the plastic load P_p, and the expected
ultimate load P_u, are given next. P_y is defined as the load
producing nominal yielding at the neutral axis in the web due
to shear. P_p is the load required to produce complete

plastification of the web by shear. The predicted ultimate loads were based on the tension field theory as discussed in Ref. 4.

In the final group of the table are the working load, P_w, and the maximum and minimum loads for the fatigue tests, P_{max} and P_{min}. These values will be defined subsequently in Sec. 2.3, "Test Loads."

II. TEST CONDITIONS

2.1 Setup

The test setup used is shown in Fig. 1. The girders
were supported at the quarter points and loads were applied
at each end. This arrangement provided a uniform, high
shear between the supports (Fig. 2) and released the test
section from stress concentrations due to load application.

In order to prevent tilting of the girders, 2 1/2-inch
standard pipes were pin-connected at one end to all inter-
mediate stiffeners near the compression flange and at the
other end to a stiff crossbeam. A supporting pipe was also
used at each loading stiffener adjacent to the loading jack.
All pin connections were such that lateral movement could be
minimized and the girders could deflect freely in the vertical
direction under the anticipated loads.

To ensure stability of the entire system, supports and
loading jacks were fastened to the test bed or to the frames
which in turn were bolted to the test bed. Figure 3 gives a
general view of the setup and loading equipment which is
described next.

2.2 Loading Equipment

For both static and cyclic loading, two 110-kip capacity Amsler jacks were used. These jacks are hydraulically operated. They have lapped ram pistons with maximum strokes of 5 in. and 0.44 in. for static and cyclic loading, respectively. Spherical seating at both ends of the jacks assures proper loading bearing.

Each jack was connected to an Amsler pulsator which provided the oil pressure. A description of the functioning of the pulsators (as well as the loading jacks, the supporting frames, and the test bed) is given in Ref. 7. Basically, these units consist of a pump, which produces a constant pressure in a cylinder for static load, and a mechanically adjustable piston in the cylinder to produce a sinusoidal variation of the pressure through the cylinder to the jacks for cyclic loads. Maximum and minimum pressures are measured directly at the piston of the jack and are indicated at gages mounted on the pulsators.

The two pulsators were coupled together for the tests to assure equality of load magnitude and synchronization of load application. This was done by connecting the crank shafts and the two pressure cylinders in parallel so that the pulsators actually acted as one unit. An operating speed of 250 cycles per minute was used for cyclic loading.

2.3 Test Loads

The procedure used to determine the test loads is best explained with the help of a modified Goodman diagram,[8] Fig. 4a. Because loads, not stresses, were to be specified, the scale of the ordinate and abscissa of the diagram is in units of force instead of stress. The ordinate gives the maximum load, the abscissa the minimum load. The predicted static ultimate load P_u, was plotted as point A in the diagram. Point B on the vertical axis was located by assuming that the static working load, designated P_w, is in the same ratio to P_u as the allowable working stress is to the yield stress. Thus, with 18 ksi for the allowable working stress and 33 ksi for the yield stress, the magnitude of P_w is

$$P_w = \frac{\sigma_w}{\sigma_y} P_u = \frac{18}{33} P_u = 54.5\% \ P_u$$

With a straight line between points A and O as the minimum load line and a straight line between points A and B as the maximum load line, the diagram was completely determined.

By the definition of the modified Goodman diagram, any load range in the diagram should result in the same fatigue endurance. Though it should not matter whether a range of O to P_w or from half-maximum to maximum was chosen, the latter range was used because it was considered to be closer to

actual field conditions than is the 0 to maximum range. This

gave a maximum load of 70.6 percent of P_u or 130 percent of

P_w and a minimum load half as large. The test loads for

girder F2 were so determined and are shown in Fig. 4c.

For the diagram applicable to girder F1 (Fig. 4b), the

reasoning used for girder F2 to determine the load range of 0

to maximum does not apply. The preliminary computation of

reference loads contained an error which resulted in a some-

what arbitrary location of the maximum load line. Thus a

half-maximum to maximum range of 41.7 to 83.4 percent of P_u,

or 76.4 to 153 percent of P_w, was used. As a result, the

range for F1 was much more severe than that applied to girder

F2 and a pronounced difference in the fatigue life of the two

girders was to be expected. Nevertheless, since fatigue life

was unknown before testing and the load range of 0 to P_w in

the modified Goodmen diagram was arbitrarily assumed anyway,

the inconsistency may be the only consequence of the error.

2.4 Sequence of Testing

With the idea that the girders might sustain more than

two million cycles of the test loads, it was planned to have

two stages of loading for each girder: first, two million

cycles of the test loads; then testing to failure with a range

of 55 kips to 110 kips, the capacity of the loading equipment.

Static tests with loads up to P_{max} were to be conducted
prior to any cyclic loading and after each million cycle
increment. The initial static test was needed to absorb the
inelastic (residual) deformations that occur on first loading,
to obtain deflection data for computing the inertia effect
due to dynamic loading, and to perform static observations.
The results of these observations, when compared with those
obtained from subsequent static tests, were expected to show
the effect of fatigue loading on the static behavior of the
specimen.

The actual testing sequence for each girder is depicted
in Fig. 5 and will be discussed in Section 3.1. As can be
recognized from the figure, the planned sequence was in-
terrupted for repairs and even changed after a repair. The
repair of a panel permitted continuing the test on other
panels and thus provided more information from the tests.

2.5 Instrumentation

The only instrument measurement made during cyclic load-
ing was the maximum end deflection, which was recorded by a
mechanically operated slip gage. Any significant damage to
the girder would result in a greater end deflection and
would be indicated to the nearest thousandth of an inch by
the dial mounted on the slip gage.

During static tests, three types of instrument observations were made. Strains in the test panels were recorded by electrical resistance strain gages (SR-4, Al) bonded to the webs in rosettes. Lateral web deflections were measured by a dial gage rig specially designed for this purpose.[2] Girder deflections were determined by a dial gage at one end and by an engineer's level and scales. The locations where the strain gage and web deflection measurements were taken are shown in Fig. 6 along with the coordinate system used throughout the tests and this report.

During the tests, visual observations were made to detect hair cracks in the girders. Careful inspection was facilitated by using a magnifying glass, especially at short time intervals during cyclic loading. Loading and supporting frames, lateral supports, and the loading system were observed constantly to ensure safe and smooth testing.

III. TEST RESULTS

In the following the results of the tests are summarized. Reference is made to Fig. 5 for the sequence of testing and to Fig. 6 for the coordinate system used.

3.1 Crack Development and Repair

A. Girder F2

Girder F2 had an aspect ratio of 1.0 and was the stronger of the two girders. Therefore, it was tested first to check the setup and the loading equipment. Testing proceeded as planned up to two million cycles with a load range of $0.35 \ P_u$ to $0.71 \ P_u$ (46.5 to 93 kips) and with static tests to the maximum load of 93 kips at zero and one million cycles. No fatigue cracks had been observed anywhere in the test section up to this point.

The second step of testing was initiated with a static test to 110 kips, the jack capacity and the anticipated maximum load of the subsequent load range. A careful inspection at this load revealed a pair of hair cracks at the web toe of the fillet welds along the stiffener at $x = -25$, as shown in detail A of Fig. 7. These cracks were only visible on the near side of the web (positive z direction). Since they were only hair cracks less than 3/16-inch deep, an attempt was made as an experiment to repair by placing

weld beads over the cracks. It was thought that the welding
might close up the cracks and peening might redistribute the
residual stresses to a more desirable condition. After weld-
ing, cyclic loading was then resumed with a load range of
46.5 kips to 93 kips.

At about 2,070,000 cycles (about 70,000 cycles after
welding), it was apparent that the attempted repair was not
successful since some hair cracks became visible either
through the weld beads or along the edges of them. At
2,500,000 cycles, these cracks had penetrated through the
web and started to propagate both upward and downward.
Also, a new crack of a similar nature had developed along
the same stiffener sixteen inches above the girder's longi-
tudinal axis. Before excessive propagation of cracks, the
test was stopped and, after observations at 93 kips, the
stiffener at x = -25 and the cracks along it were isolated
by welding a pair of reinforcing stiffeners on each side of
the stiffener and 7 1/2 inches away as shown in Fig. 7.

The reinforced girder then had one original panel with
an aspect ratio of 1.0, two stronger panels with α = 0.85,
and two isolated portions with α = 0.15. Increasing the load
range to 55 kips to 110 kips (41.9 to 83.8 percent of P_w),the
test was continued after a static test to 110 kips. A new
hair crack was discovered when about 580,000 cycles had

elapsed (3,080,000 total, in different ranges). It was located

near the longitudinal axis of the girder and at the web toe of

the fillet weld along the stiffener at x = +75 (Fig. 7,

detail B). Again, the crack was only visible from one side

of the web, the far side this time. Later, at about 608,000

cycles after increase of load (3,108,000 total), another

small crack developed just above the previous one (Fig. 7,

detail B). These cracks were observed for a while and the

test terminated at 3,277,000 total cycles because of cracks

at the ends of the cover plates outside the test section.

Since the behavior of partial length cover plates under

fatigue is not within the scope of this investigation, it

will not be discussed here.

B. Girder F1

Before consideration of the details of crack develop-

ment of girder F1, it should be recalled that this girder

had an aspect ratio of 1.5 and was tested with a load range

of 41.7 to 83.4 percent of P_u (44 to 88 kips), more severe

than that for girder F2.

After the initial static test and about 330,000 cycles

of load, a crack was noticed at the web toe of the fillet

weld along the top flange. It was a few inches long and

visible from both sides of the girder. Because of the

relatively rapid rate of crack propagation, the test was

brought to a stop. Static observations at 88 kips were then

made and the crack length thus obtained is shown in detail
A of Fig. 8. Other than this crack, no visible damage was
detected on the girder.

In similarity to the procedure used before on girder F2,
the failed part was isolated by adding a pair of stiffeners
at x = -20 to permit further loading cycles. Prior to the
welding of this pair of reinforcing stiffeners, however, the
metal around the crack was first removed with an air-operated
gouge and weld beads were then deposited, resulting in a
heavier fillet weld in this area (Fig. 9a). With the rein-
forcing stiffeners, the new panel had an aspect ratio of 1.1
as compared to the neighboring original panel of 1.5.

Following the repair, a static overload to 95 kips was
applied to redistribute the residual stresses introduced by
welding around the crack. Testing was then resumed with the
same range of loading as before and continued to 1,850,000
(total) cycles, only stopping for a static test at 1,000,000
cycles according to plan. At 1,850,000 cycles, testing was
discontinued because of propagation of a crack which first
appeared on one side of the web along the stiffener at x = 0
at 1,200,000 cycles and then penetrated the web, growing to
the stage shown in detail B of Fig. 8.

On girder F2 an unsuccessful attempt had been made to
repair a crack by merely depositing weld beads over it. To
investigate another possibility, the procedure applied
earlier to the crack along the top flange was used. The
metal along the crack was first gouged out from one side of
the web and weld beads deposited, then gouged and welded on
the other side of the web. A horizontal section through
the repaired area would appear as Fig. 9b. Not reinforced by
stiffeners, this repair withstood a loading of more than two
million cycles to the end of the test without any visible
damage.

Again, for the purpose of redistributing residual
stresses, a static overload to 95 kips was applied before
continuation of testing. Under the constant load range of
44 to 88 kips, the first crack after the repair appeared
along the top flange at 2,330,000 cycles. As all other
cracks, it was located at the web toe of the fillet weld
and was visible at first only on one side of the web. With
an increasing number of cycles, it penetrated through the
web and branched out gradually, in general perpendicular to
the tension field as can be visualized with the aid of Fig. 8,
detail C. Other hair cracks of similar shape also developed
in the same general area and gradually joined each other.
By 3,780,000 cycles, a small crack began to appear along

the stiffener at x = +75, about 8 in. below the top flange
(Fig. 8, detail C). From then on, while the cracks grew, many
new hair cracks could be detected along the boundaries of the
long panel, in the general vicinity of the tension field. A
visual inspection under static load was made at 4,000,000
cycles.

When cyclic loading was resumed, the two major cracks
described in the last paragraph continued to propagate at a
faster and faster rate because the effective area for tension
field action was reduced more and more. The final failure
occurred at 4,077,000 cycles when the crack branching out
from the top flange joined the crack along the stiffener at
·x = +75 and the web was ripped apart. This failure is shown
in Fig. 10.

3.2 Effects of Cyclic Loadings on Static Behavior

Considering fatigue testing of a piece of metal under
simple tension or shear, one may be able to predict that no
change of strain pattern could be measured by mechanical
devices unless fatigue failure is well under way. Such a
concept should also apply to the fatigue testing of a welded
plate girder even though the pattern of residual stresses,
the state of applied strain, and redistribution of stresses
near hair cracks make the strain distribution complicated.
All the instrument observations in the tests generally

confirmed this. Since the situation is similar for both girders F1 and F2, the discussion for one generally applies also to the other.

A. Girder Deflection

Figure 11 shows the observed vertical deflections of girder F2 for two different static tests but under the same loading condition. Both curves correspond to the maximum applied load for the girder, 93 kips. The upper one is obtained from data taken before any cyclic loading; the lower one is obtained after two million cycles. A comparison of the two curves indicates that little change in girder deflection was caused by the two million cycles of loading, which was just sufficient to cause a hair crack in the web.

As another example, the maximum end deflection of girder F1 with respect to its support is plotted in Fig. 12 against the number of cycles of loadings applied to the girder. The occurrence of cracks and repairs by welding are also indicated in this figure (also refer to Fig. 5). It can be visualized that only when an appreciable amount of cracking was observed did the deflection increase slightly. The final, sudden deflection, of course, corresponded to the complete destruction of the web (Fig. 10).

B.   Web Deflection

To describe the behavior of a girder web under cyclic
loading, two cross sections of girder F2 are shown in Fig. 13.
The deflected cross-sectional shapes are approximated by
connecting the measured positions of web points with straight
lines. (The web deflection shapes, the girder deflections
discussed before, and the stresses in the web are all similar
to those obtained from test girders G6 and G7, Ref. 2).
During the fatigue testing, the web fluctuated back and forth
between the shapes shown under maximum and minimum loadings.
At some locations, such as the lower parts of the sections,
the range of fluctuation was ~~half an~~ 0.2 inch or more.

Even with fluctuations of such magnitude, and with cracks
along panel boundaries, the web deflection under a given load
remained practically unchanged throughout the tests. This is
borne out by the two almost identical deflection shapes under
maximum loads in each cross section of Fig. 13. The approxi-
mate shapes with heavier lines correspond to loads before any
cyclic loading and the adjacent shapes with thinner lines are
obtained after application of two million cycles (at $x = 0$)
or after cyclic testing was completed (at $x = +50$).

C.   Membrane Stresses in Web

If any detectable change in web strain resulted from
cyclic loadings, the principal membrane stresses would change

accordingly. However, changes were so small that they were
hardly significant. Principal membrane stresses for maximum
loads at points along the section x = +37 1/2 of girder F1
(Fig. 6) are shown in Fig. 14. Data for these stresses were
obtained from strain gage rosettes and reduced by using Mohr's
circles. With web failure and repair in the neighboring panel
between zero and one million cycles, and cracking of the web
along the left hand stiffener in this panel (Fig. 8), there
were only slight changes in the magnitude and orientation of
these stresses. In other words, changes in the tension field,
if any, due to hair cracks in a web panel cannot be clearly
measured (unless a crack is adjacent to a strain gage).
Naturally, when cracks grow to a stage where they hinder the
tension field action, the principal membrane stresses are
affected and hence the girder strength changes.

IV. DISCUSSION AND CONCLUSIONS

The fatigue tests on girders Fl and F2 were intended to investigate the applicability of the design recommendations[1] to bridge girders, to proof-test the setup and loading equipment, and to serve as a basis for planning further tests. It is evident that the loading equipment and setup were safe for the loads used. A more analytical study with suggestions for further investigations will be presented in a later report.

The test section of girder F2 had a web slenderness ratio of 263 and three test panels each with an aspect ratio of 1.0, a value just about the recommended limit of $(260/263)^2$. These panels sustained two million cycles without the development of any visible fatigue cracks although the load range was 65 to 130 percent of the proposed working load for AASHO Specifications. By the modified Goodman diagram, this would mean that the girder could sustain for two million cycles a load range of 0 to working load, which is much more severe than the usual load condition on highway bridges.

The test section of girder Fl has about the same web slenderness ratio (265), but only two identical test panels. The panel length was 1.5 times the web depth, far beyond the limiting value of $(260/265)^2$ as permitted by the design recommendations.[1] Also the load range was proportionally higher than for girder F2, varying from 76.4 to 153 percent

of the proposed working load for highway bridges or equivalent
to a load range of 0 to 1.2 times the working load according
to the modified Goodman diagram. On this girder a crack was
observed in one panel at one third of a million cycles while
another panel stood for 1.2 million cycles before the first
hair crack was detected. With repairs, a total of about four
million cycles was applied without any drastic effect.

*if the assump-
tion*

For these two shear girders where tension field action
developed, the test results lie in the same general domain
as other fatigue tests on welded plate girders or beams:
depending on the loading range and its relation to the strength
of the specimen, the fatigue life can be long or relatively
short. Certainly, results of laboratory fatigue tests in
general cannot be directly applied to performance in the field,
even when full size specimens are used for testing. The
variation of load magnitude and distribution and the random
frequency of occurrence may be far from the loading pattern
applied in testing. Nevertheless, since the tension field
action under a very severe loading condition in these tests
apparently did not lead to a more severe fatigue problem
than those which existed in the past under other loading
conditions, and since the time-tested AASHO reduction in
allowable stress (for A7 steel, from 20 ksi to 18 ksi, or
10 percent) would be used for highway bridge girders, the
design recommendations[1] with the corresponding stress re-
duction appear to be safe for highway bridges.

ACKNOWLEDGEMENTS

NOMENCLATURE

α - Aspect ratio = Panel length/web depth

β - Web slenderness ratio = Web depth/web thickness

τ_{cr} - Critical (buckling) shear stress

σ_w - Allowable working stress in bending

σ_y - Bending yield stress

I - Moment of inertia of a cross section

P_{cr} - Buckling load according to linear buckling theory

P_{max} - Maximum load of cyclic loading

P_{min} - Minimum load of cyclic loading

P_p - Plastic load, causing plastification of web by shear

P_u - Predicted static ultimate load

P_w - Static working load $= \dfrac{\sigma_w}{\sigma_y} P_u = \dfrac{18}{33} P_u = 0.55 P_u$

P_y - Load producing nominal shear yielding at neutral axis in web

Q - First moment of the cross-sectional area above or below the neutral axis taken about the same axis

S - Section modulus of a cross section

x,y,z - Coordinate system as shown in Fig. 6

GIRDER	COMPONENT	DIMENSIONS (in)
F1	Top Cover Plate	11.06 x 0.989
	Top Flange	12.04 x 0.995
	Test Web	50 x 0.189
	End Web	50 x 0.389
	Bottom Flange	12.02 x 0.998
	Bottom Cover Plate	11.06 x 1.007
F2	Top Cover Plate	11.09 x 0.991
	Top Flange	12.00 x 0.998
	Test Web	50 x 0.190
	End Web	50 x 0.389
	Bottom Flange	12.02 x 0.995
	Bottom Cover Plate	11.09 x 0.990

Table 1   Cross-Sectional Dimensions

Designation			Chemical Analysis				Coupon Tests			Remarks
Location	Thick-ness (in.)	Coupon	C %	Mn %	P %	S %	σ_y (ksi)	σ_u (ksi)	Elong. %	
Girder F1										
Top Cov.	1	CPF1	.18	.72	.010	.019	32.5	66.5	30.9	
Top Flg.	1	CPF3	.17	.73	.012	.026	32.4	63.7	33.4	Also for Bottom Flange & Cover Pl
End Web	3/8	CPF4	.19	.52	.011	.030	33.4	61.2	30.4	
Test Web	3/16	CPF5	.22	.68	.030	.027	34.8	62.2	27.1	
Test Web	3/16	CPF5A	.22	.68	.030	.027	36.1	64.7	21.2	Transverse
Girder F2										
Top Cov.	1	CPF10	.18	.72	.010	.019	32.3	67.0	31.0	Also for Bottom Cover Plate
Top Flg.	1	CPF12	.17	.73	.012	.026	30.3	62.9	32.0	Also for Bottom Flange
End Web	3/8	CPF13	.19	.52	.011	.030	34.6	60.1	25.7	
Test Web	3/16	CPF14	.22	.68	.030	.027	34.6	62.3	27.1	
Test Web	3/16	CPF14A	.22	.68	.030	.027	35.0	62.9	23.3	Transverse

Notes: All plates conform to ASTM A373-58T

Table 2   Material Properties

Step	Connection	Position*	Weld**
(1)	3/8" web plates to 3/16" web plate	NS	(a)
(2)	3/8" web plates to flanges	NS	(b)
(3)	3/16" web plates to flanges	NS	(c)
(4)	Same as (1)	FS	(a)
(5)	Same as (2)	FS	(a)
(6)	Same as (3)	FS	(c)
(7)	Bear. stiff. to 3/8" web plates	FS	(d)
(8)	Inter. stiff. to 3/8" web plates	FS	(e)
(9)	Inter. stiff. to 3/16" web plate	FS	(c)
(10)	Same as (7)	NS	(d)
(11)	Same as (8)	NS	(e)
(12)	Same as (9)	NS	(c)
(13)	Ends of cover plates to top flange	TS	(f)
(14)	Center 46" of cover plates to top flange	TS	(f)
(15)	Rest of cover plate to top flange	TS	(g)
(16)	Ends of stiff. to bottom flange as required	TS	-
(17)	Ends of cover plates to bottom flange	BS	(f)
(18)	Center 46" of cover plates to bottom flange	BS	(f)
(19)	Rest of cover plates to bottom flange	BS	(g)
(20)	Ends of stiff. to top flange as req'd	BS	-

*   NS, FS, TS, BS indicate near, far, top and bottom sides, respectively, were topmost

** See Table 3b for weld sizes and welding details

Table 3a Welding Sequence

Size		Detail
Butt	(a)	Sub. Arc, 425 amps-30 volts, 5/32 Hi Mn Wire, 35 in./min.
1/4 fillet	(b)	Sub. Arc, 650 amps-29 volts, 5/32 Hi Mn Wire, 29 in./min.
1/8 fillet	(c)	Manual, 125 amps-60 volts, D.C., E6012 rod - 1/8 ∅
1/4 fillet	(d)	Manual, (other information not available)
3/16 fillet	(e)	Manual, 160 amps-60 volts, D.C., E6012 rod - 5/32 ∅
3/16 fillet	(f)	Manual, 425 amps-30 volts, D.C. E6012 rod - 5/32 ∅
3/8 fillet	(g)	Same as (f) except using three passes

Table 3b Weld Sizes and Welding Details

		F1	F2
I	(in^4)	17,650	17,545
S	(in^3)	675.5	675.0
Q	(in^3)	365	365
$\alpha = \dfrac{\text{Panel length}}{\text{Web depth}}$		1.50	1.00
$\beta = \dfrac{\text{Web depth}}{\text{Web thickness}}$		265	263
τ_{cr}	(ksi)	2.72	3.61
P_{cr}	(kips)	25.7	34.3
P_y	(kips)	184.7	184.8
P_p	(kips)	191.8	192.8
P_u	(kips)	105.7	131.3
P_w	(kips)	57.6	71.6
P_{max}	(kips)	88.0	93.0
P_{min}	(kips)	44.0	46.5

Table 4   Section Properties and Reference Values
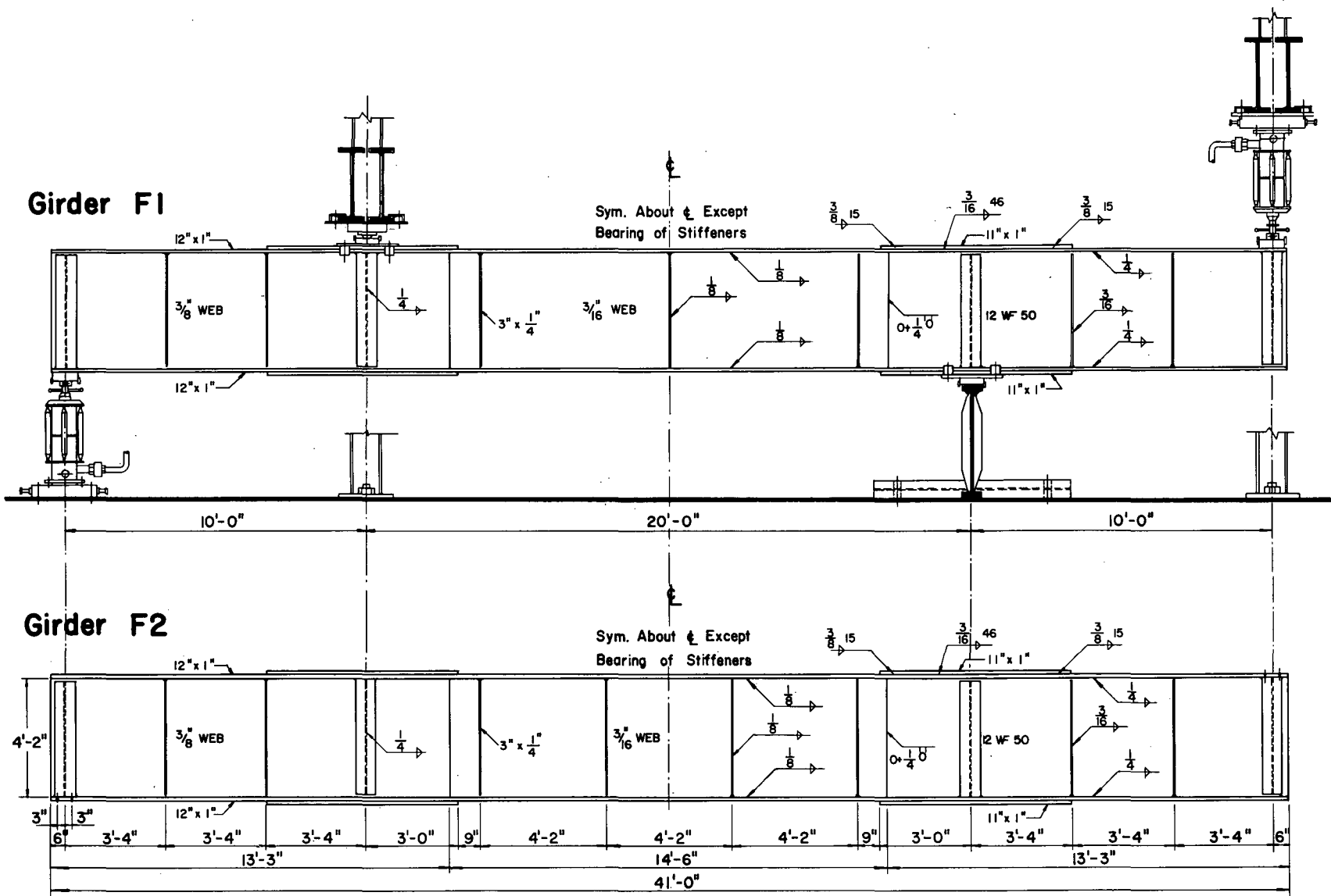
Fig. 1   Test Girders & Setup

P

P

Test
Section

P (kips)

SHEAR, V

MOMENT, M

120P (k-in.)
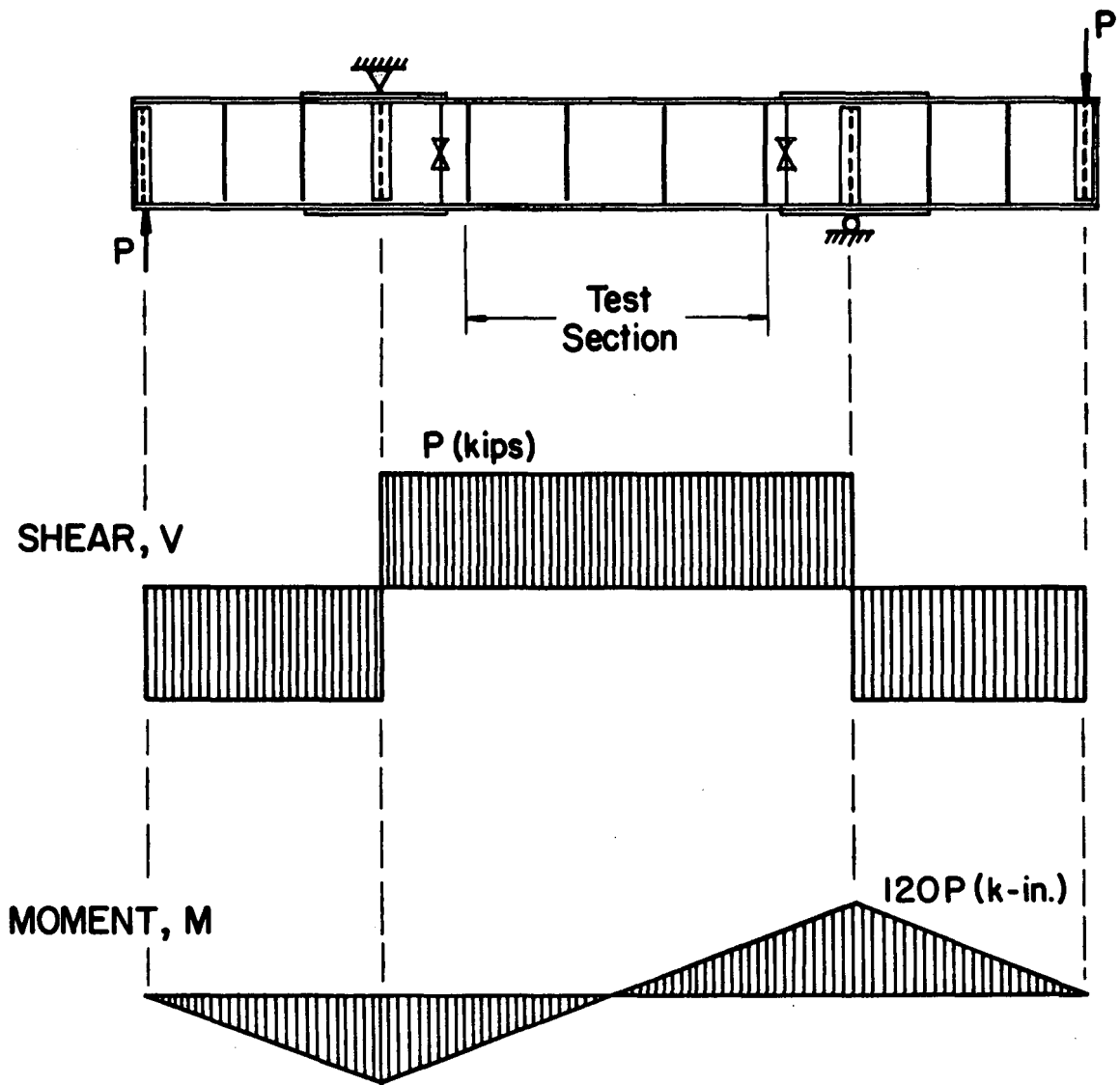
Fig. 2 Moment and Shear Diagram
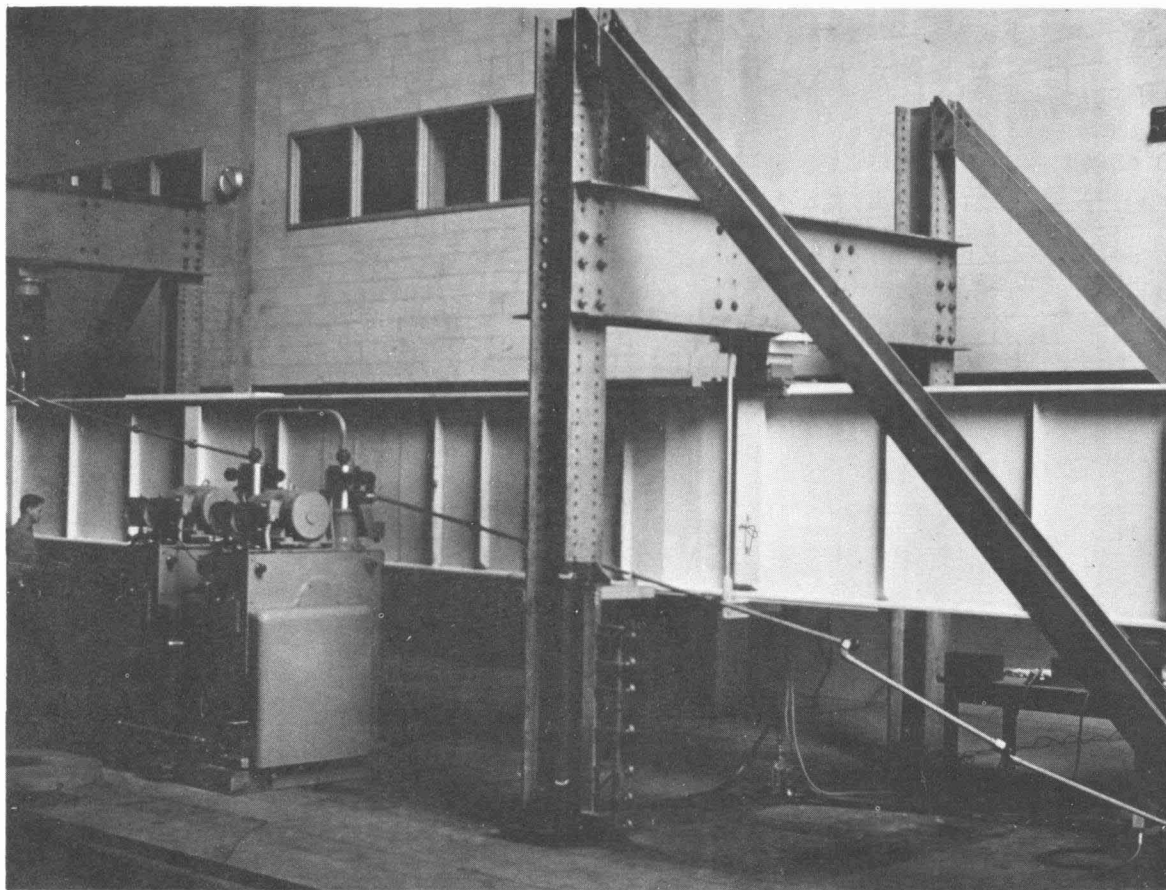
Fig. 3   Overall View of Test Setup
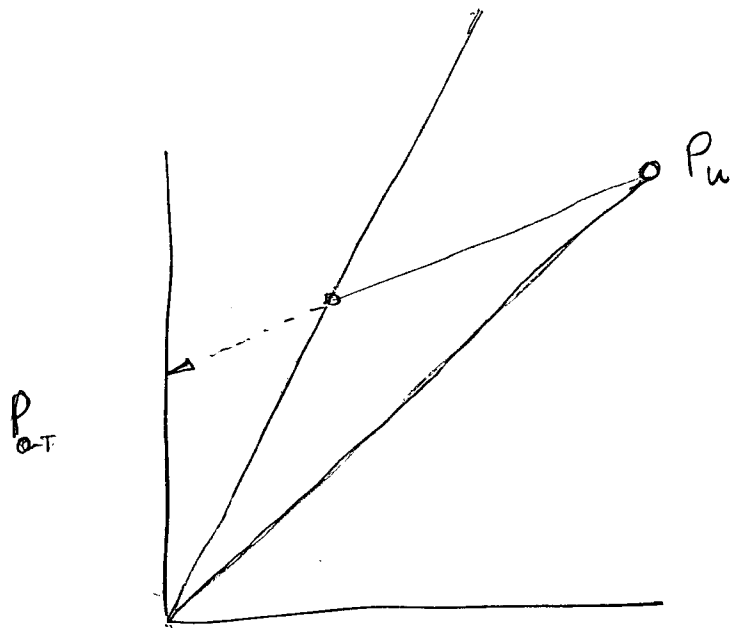
P_u

P_{Q-T}

4 a

GIRDER F 1

$P_{max} = 88^k$
$= 0.83 P_u$
$= 1.53 P_w$

4b

GIRDER F 2

$P_{max} = 93^k$
$= 0.71 P_u$
$= 1.30 P_w$

4c
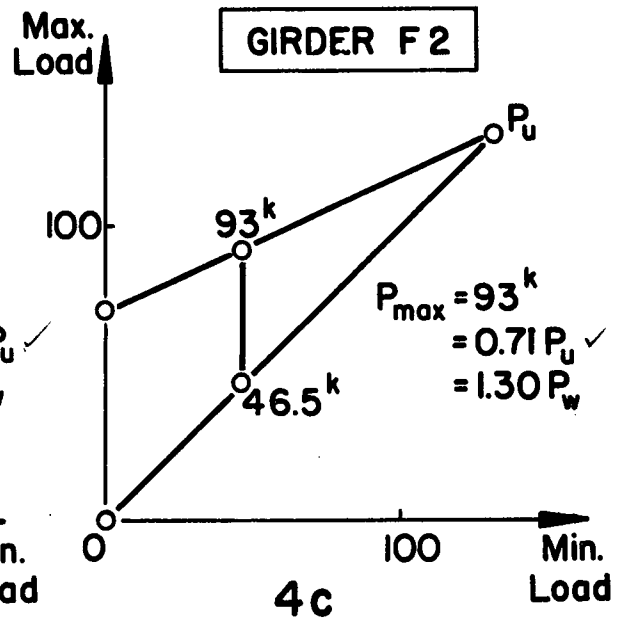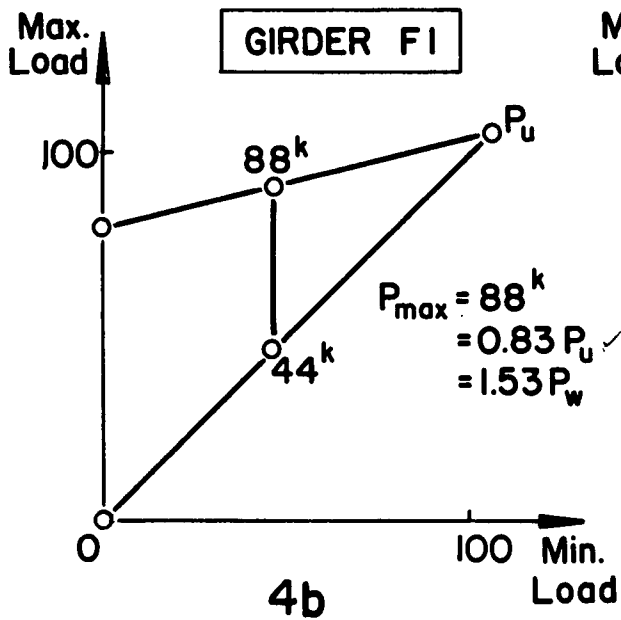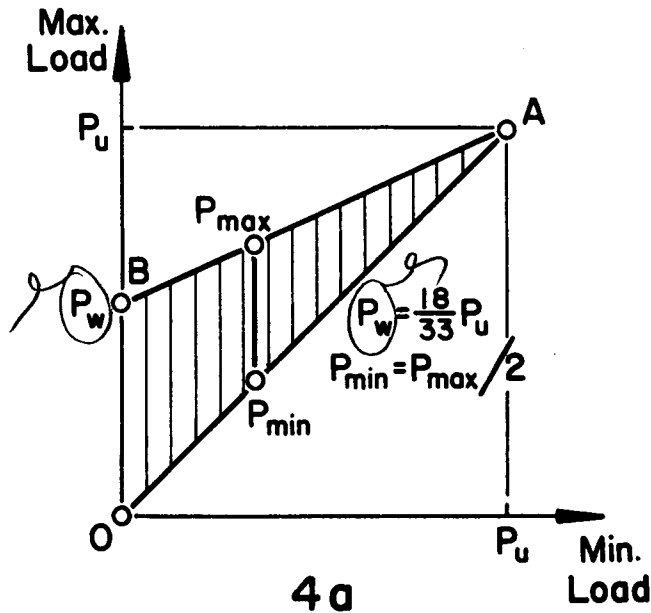
Fig. 4 Test Loads

Fig. 5 Sequence of Testing
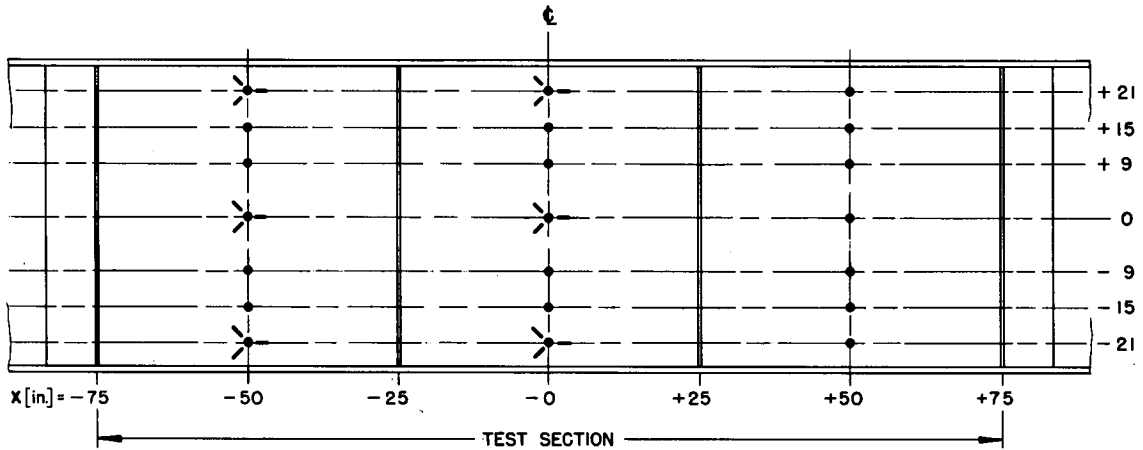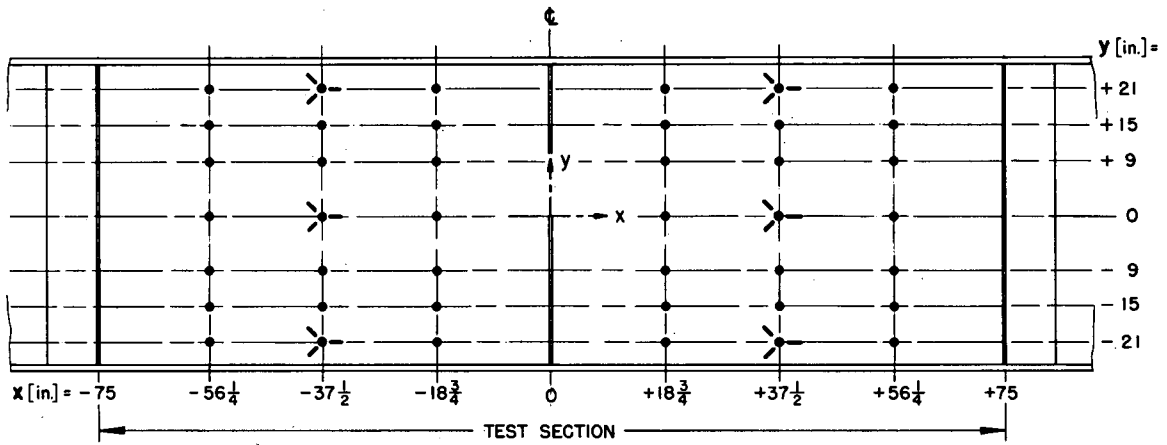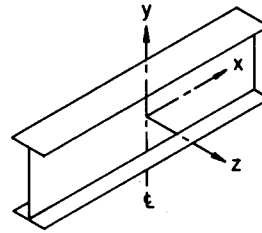
GIRDER F I

GIRDER F 2

Fig. 6 Instrumentation
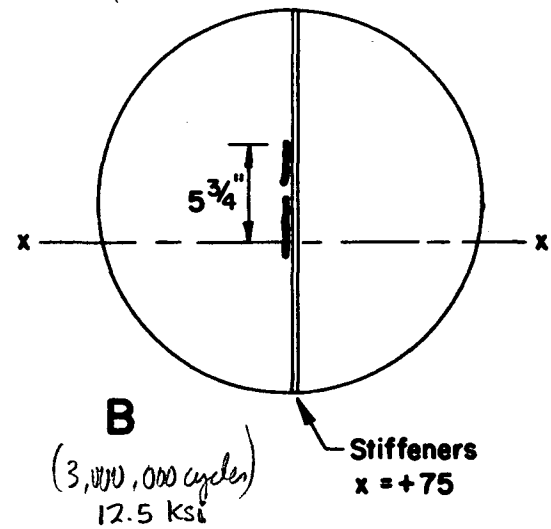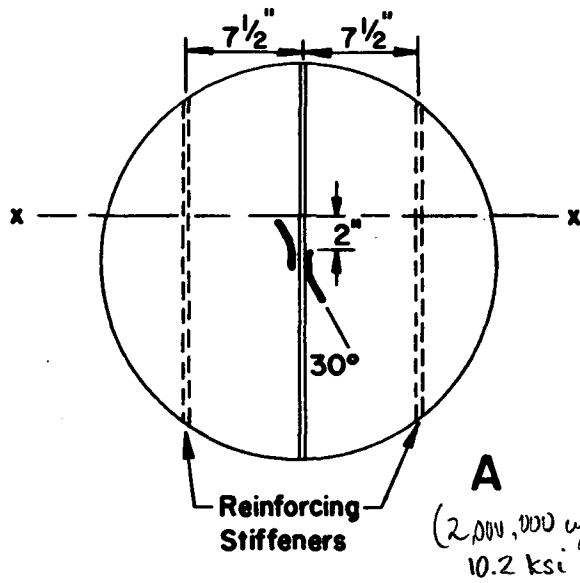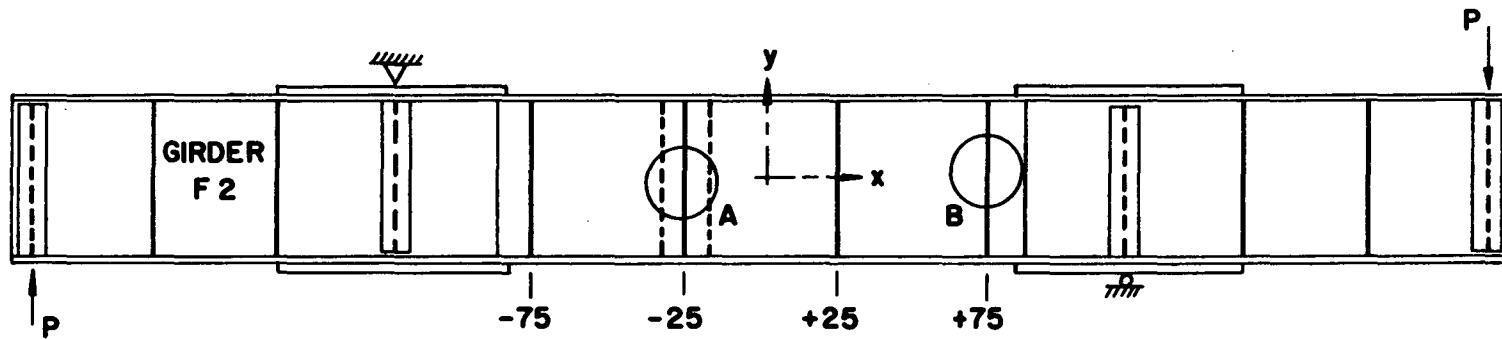
GIRDER F 2

−75 −25 +25 +75

P

7½" 7½"

2"

30°

Reinforcing
Stiffeners

A

(2,000,000 cycles)
10.2 ksi

5¾"

B

(3,000,000 cycles)
12.5 ksi

Stiffeners
x = +75

Fig. 7 Crack Location and Repairs, Girder F 2

GIRDER F1

−75 0 +75

y
A
x
B
C

P P

Reinforcing Stiffener

10" 10"

10"

8"

11"

A
9.3 ksi
0.3 million

B
8.8 ksi
1.85 million

C
13.2 ksi
3.8 million

Fig. 8 Crack Location and Repairs, Girder F1

TOP FLANGE

l"

Crack Prior
To Repair

3/16"

9a

Web

Crack Prior
To Repair

Web

3/16"

1/4"

9b

Stiffeners
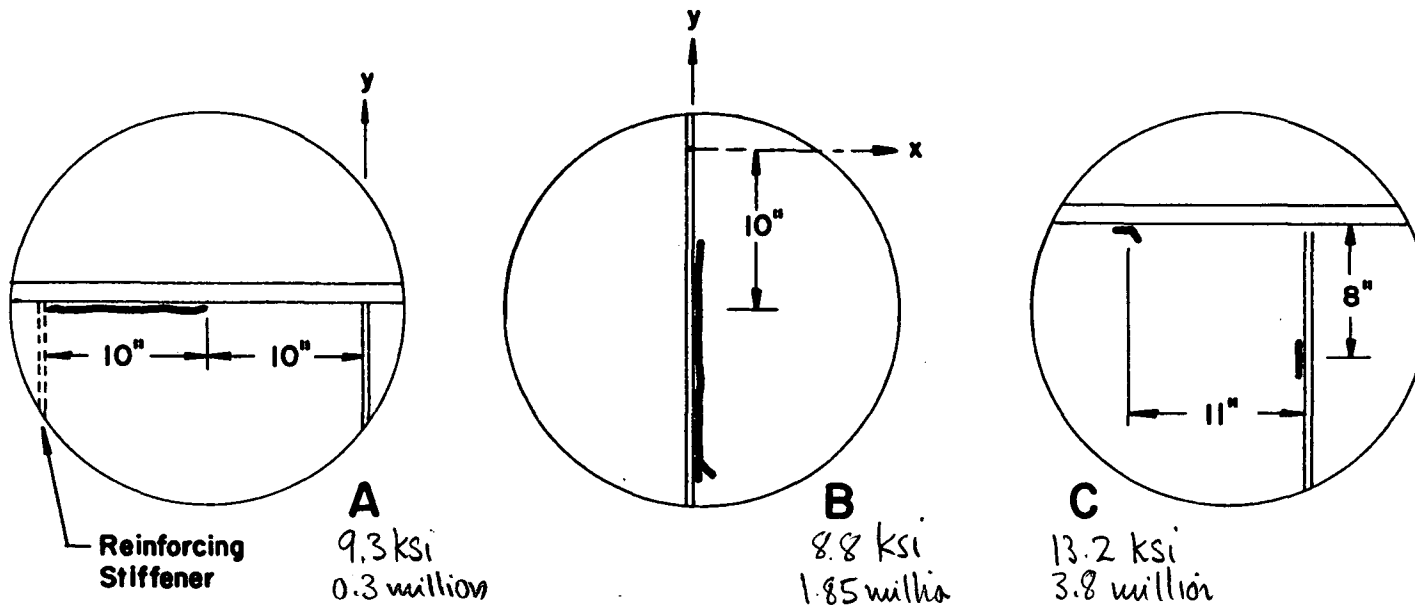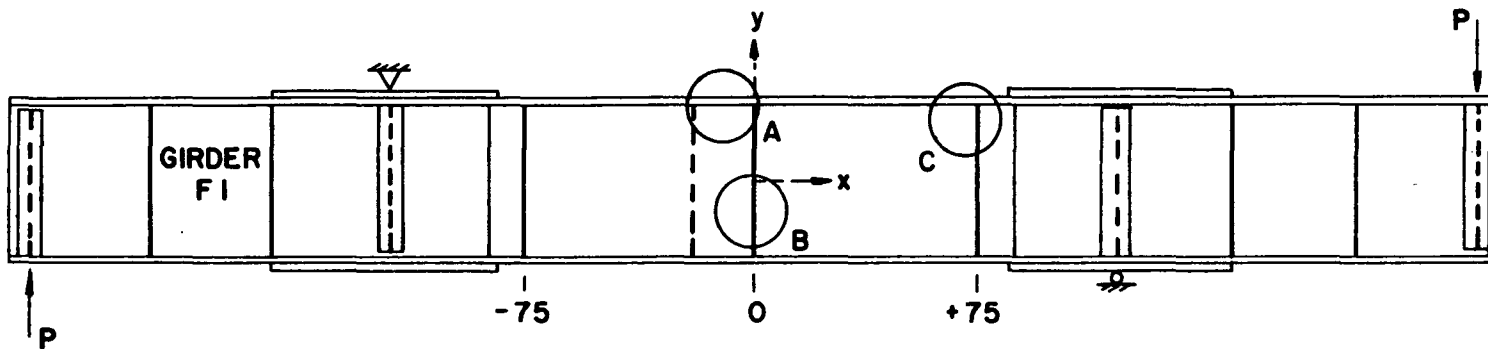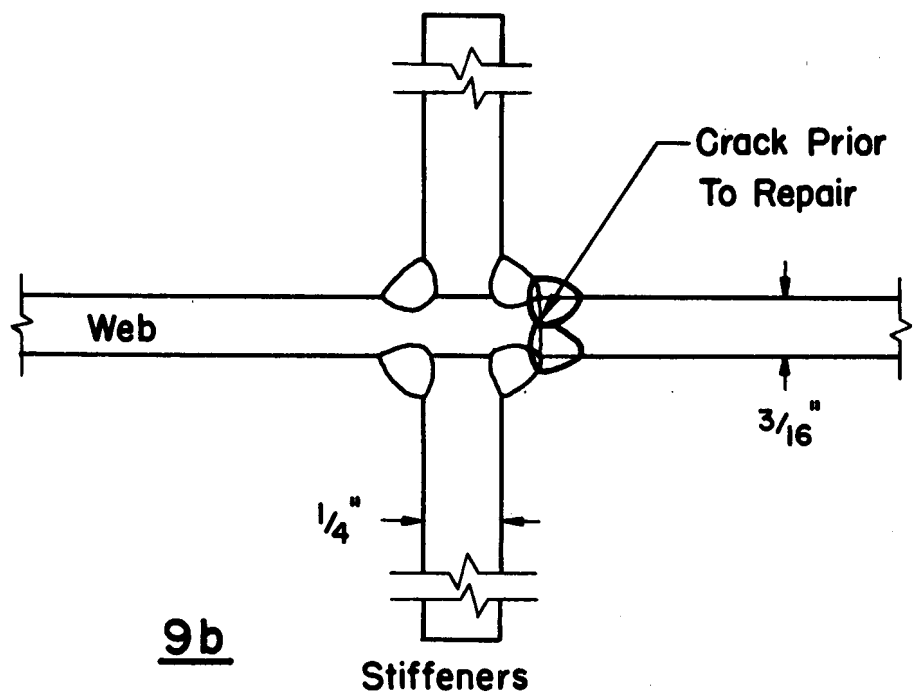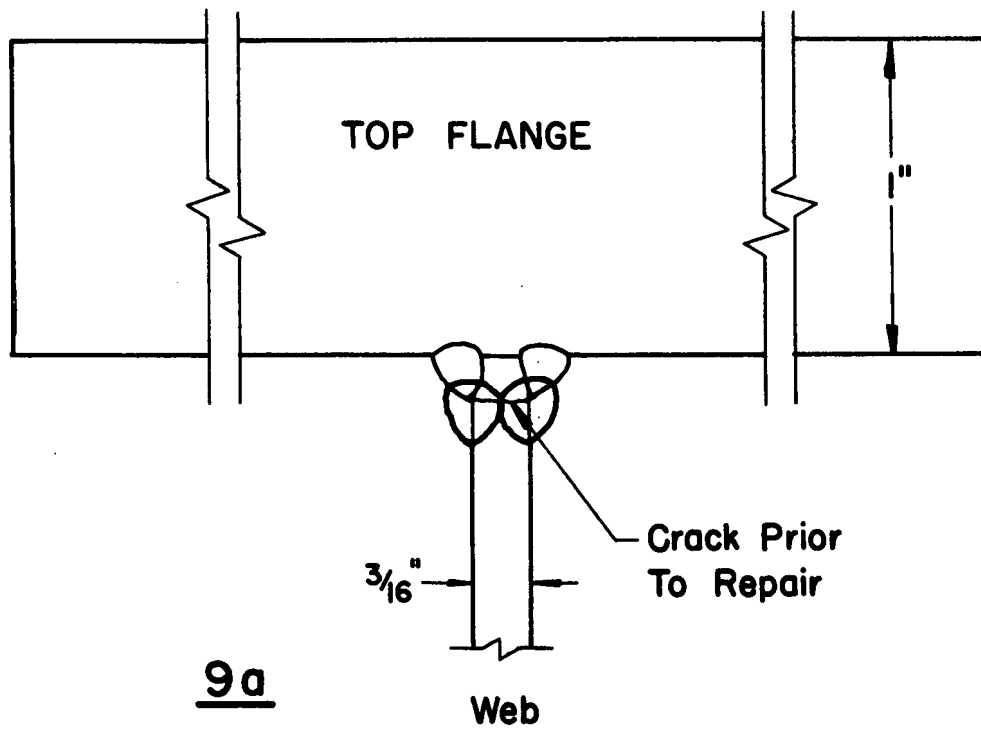
Fig. 9 Crack Repair Details
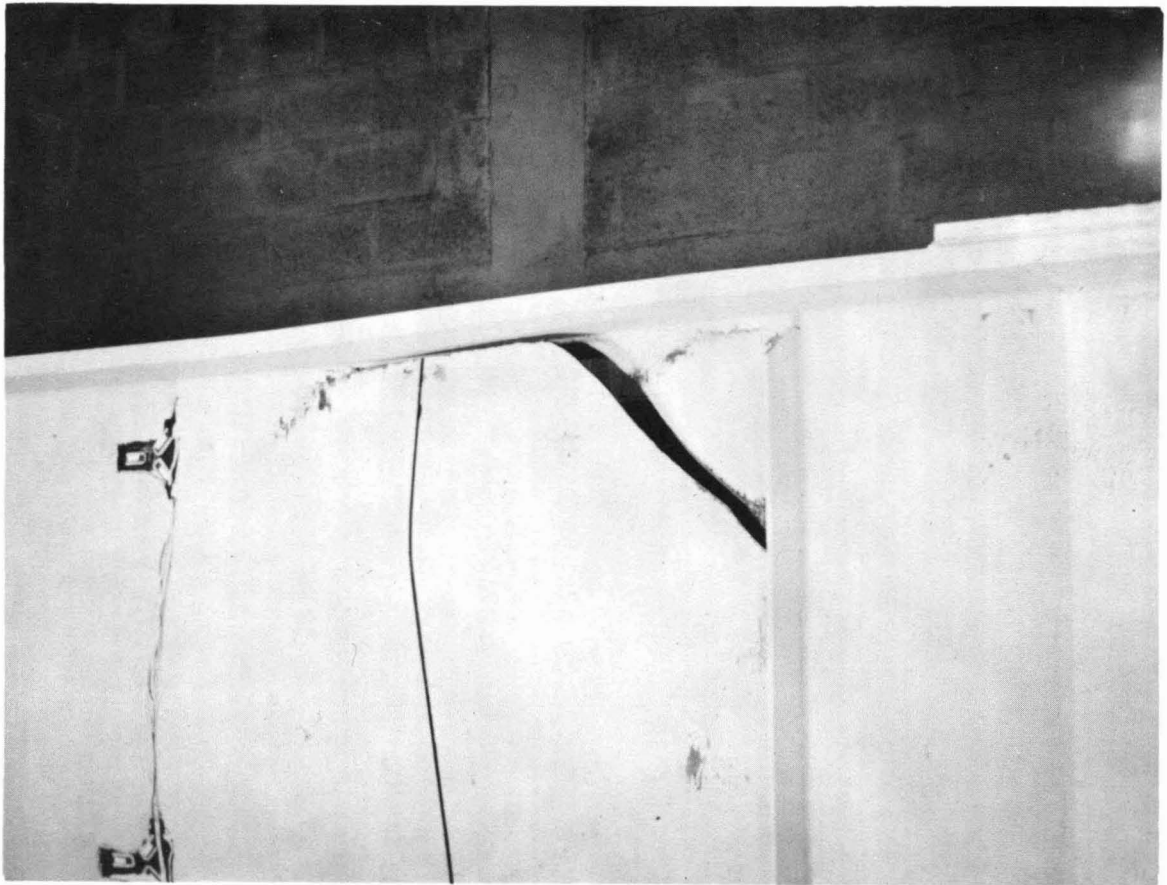
Fig. 10 Failure of Girder Fl
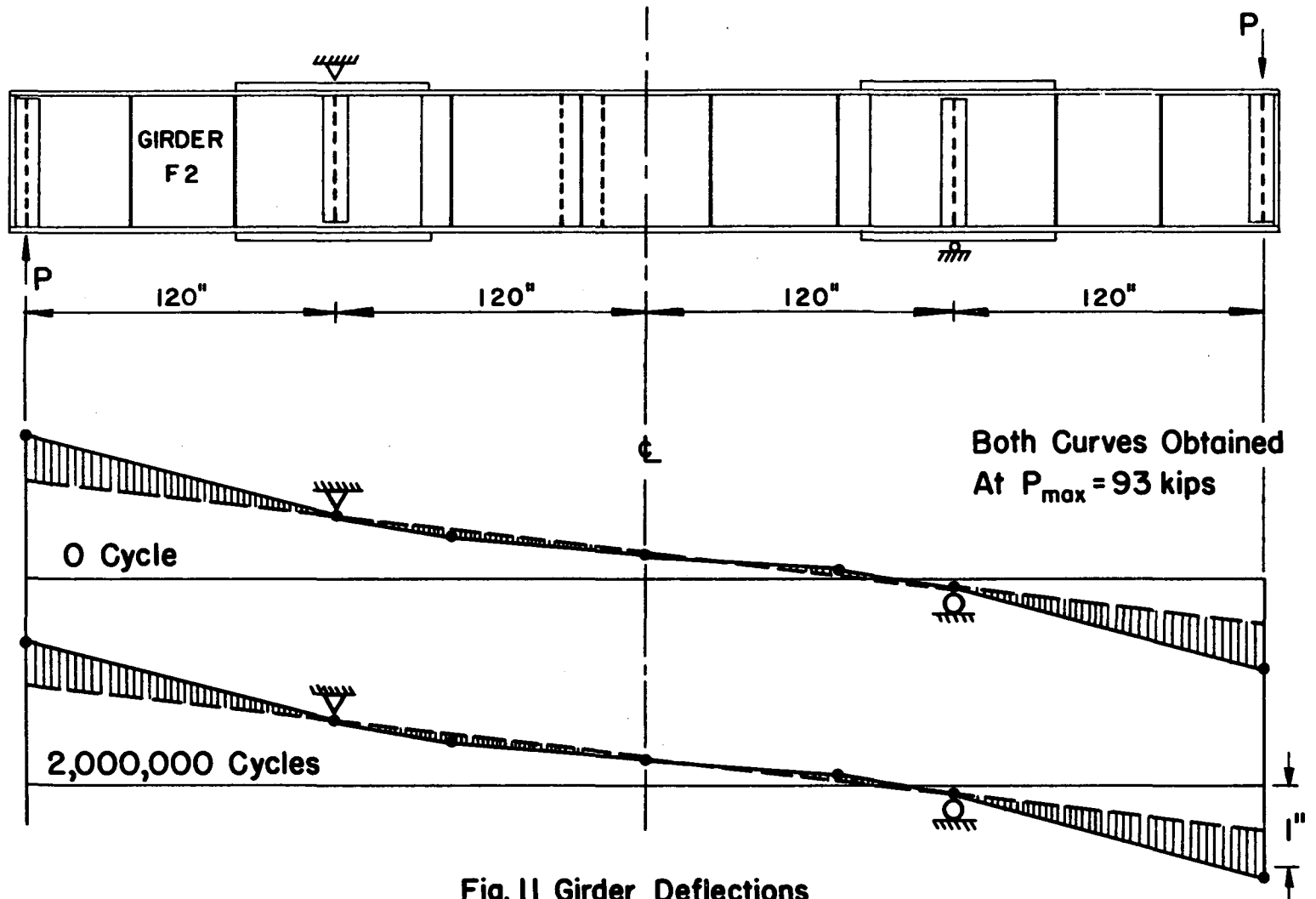
Fig. II Girder Deflections

Fig. 12 Maximum End Deflection

GIRDER F 2

$X =$ 0 +50

$P_{max.}$

$O P_{min.}$

12"

0   0.4"

$P_{max.}$

O $P_{min.}$

$X = 0$

$X = +50$

Fig. 13 Web Deflections

GIRDER F1

x=37.5

10 ksi

Compression   Tension

O

P = 88^k
10^6 cycles

P = 88^k
0 cycles

50"
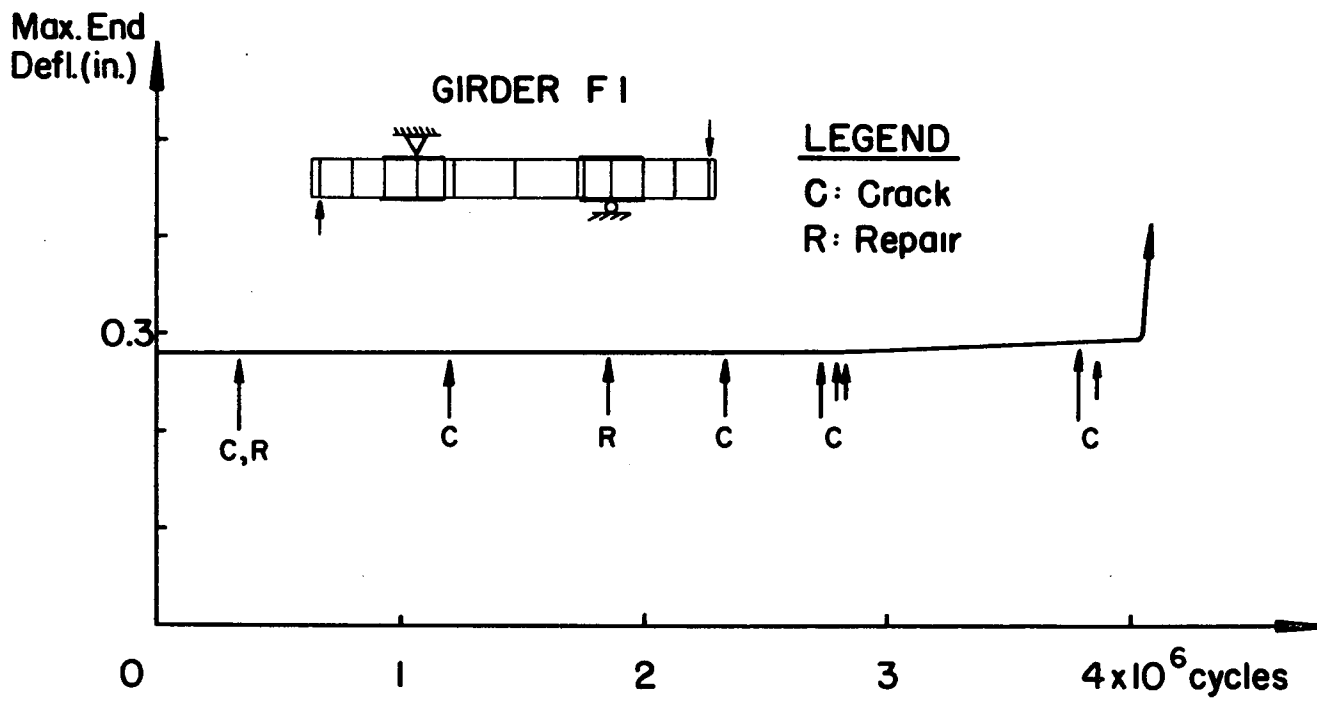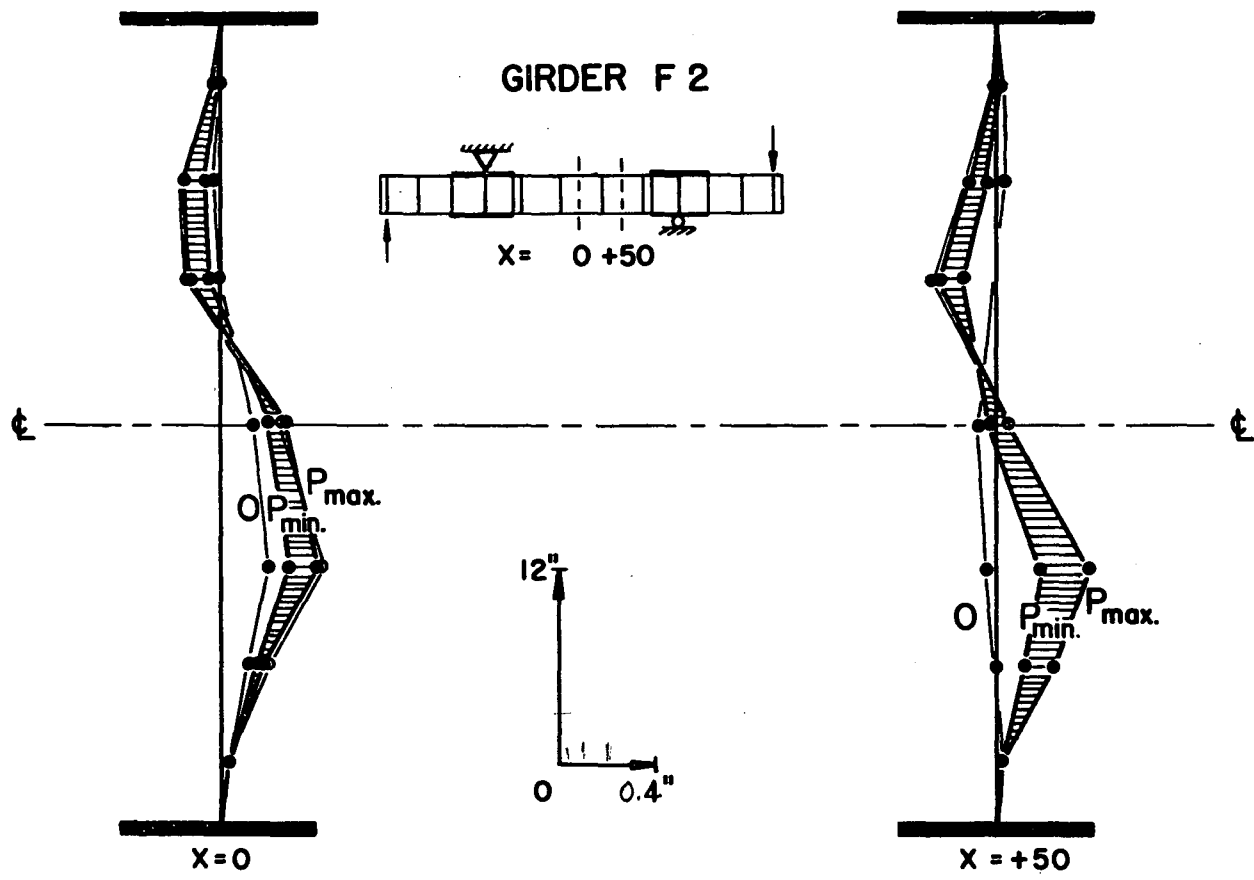
P = 88^k
1.85 x 10^6 cycles
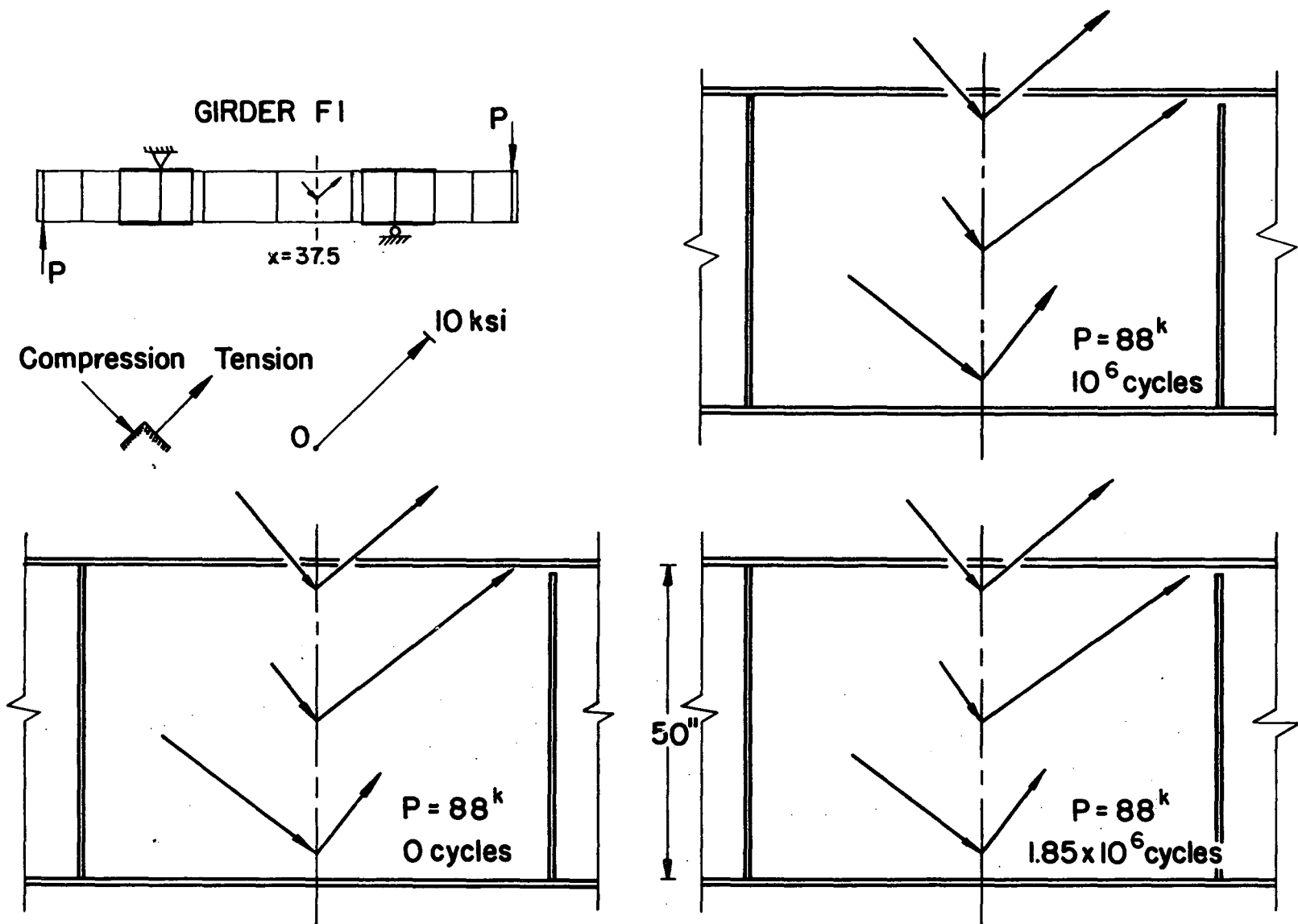
Fig. 14 Principal Stresses in Girder Web

REFERENCES

1. K. Basler
   NEW PROVISIONS FOR PLATE GIRDER DESIGN, _Proceedings_,
   AISC Nat. Engrg. Conf., 1961

2. K. Basler, B. T. Yen, J. A. Mueller, and B. Thürlimann
   WEB BUCKLING TESTS ON WELDED PLATE GIRDERS,
   Bulletin No. 64, Welding Research Council, New York,
   September, 1960

3. K. Basler and B. Thürlimann
   STRENGTH OF PLATE GIRDERS IN BENDING, _Proceedings_,
   ASCE, Vol. 87, No. ST6, August, 1961

4. K. Basler
   STRENGTH OF PLATE GIRDERS IN SHEAR, _Proceedings_,
   ASCE, Vol. 87, No. ST7, October, 1961

5. K. Basler
   STRENGTH OF PLATE GIRDERS UNDER COMBINED BENDING AND
   SHEAR, _Proceedings_, ASCE, Vol. 87, No. ST7, October,
   1961

6.   SPECIFICATION FOR THE DESIGN, FABRICATION & ERECTION
   OF STRUCTURAL STEEL FOR BUILDINGS, AISC, New York,
   1961

7. B. Thürlimann and W. J. Eney
   MODERN INSTALLATION FOR TESTING OF LARGE ASSEMBLIES
   UNDER STATIC AND FATIGUE LOADING, Proceedings, SESA,
   Vol. XVI, No. 2, 1959

8. H. J. Grover, S. A. Gordon, and L. R. Jackson
   THE FATIGUE OF METALS AND STRUCTURES, Department of
   the Navy, 1954, Revised June, 1960

DEPARTMENT OF CIVIL ENGINEERING
FRITZ ENGINEERING LABORATORY

251
April 24, 1962

TO: Members of the Welded Plate Girder Project Committee

Messrs:
E. L. Erickson   L. Grover   N. W. Morgan
A. Amirikian   T. R. Higgins   W. H. Munse
L. S. Beedle   W. H. Jameson   E. J. Ruble
K. de Vries   C. D. Jensen   J. E. South
F. H. Dill   K. Jensen   R. M. „Stuchell
E. R. Estes   B. G. Johnston   B. Thurlimann
G. F. Fox   K. H. Koopman   N. van Eenam
J. A. Gilligan   W. B. McLean   J. Vasta
                                        G. Winter

Gentlemen:

Two full-size welded plate girders were tested under fatigue loading in 1961 and some preliminary test data were presented to the committee at its last meeting. The study of the fatigue behavior of these girders will follow the same general pattern as used for the investigation of the static strength: first, a test report containing the results of the tests; second, an analytical report emphasizing the factors governing the girder strength. The enclosed report, "Fatigue Tests of Welded Plate Girders", is the first of these two reports. It is expected that the analytical report will be completed by the end of the coming summer and will be followed by a proposal for further fatigue tests.

We are submitting the report for your review and approval for publication. The main part of the report was presented orally at the ASCE Convention in Houston, but we are considering submitting the report to the Welding Research Council, which published the test report on the static strength of plate girders.

The report and its publication will be discussed at the next Committee Meeting to be held here at Lehigh University on the 29th of May. An announcement of this meeting will be made soon by Mr. C. F. Larson, the Committee Secretary.

Sincerely yours,

BTY:lm   B. T. Yen

Encl.

                                          L. S. Beedle